The Astronomical Journal, 126:1305–1311, 2003 September

FLUORINE ABUNDANCES IN THE LARGE MAGELLANIC CLOUD AND ω CENTAURI: EVIDENCE FOR NEUTRINO NUCLEOSYNTHESIS?[1,2]

Katia Cunha[3]
Observatório Nacional, Rua General José Cristino 77, 20921-400 São Cristovão, Rio de Janeiro, Brazil; katia@on.br

Verne V. Smith[3]
Department of Physics, University of Texas at El Paso, El Paso, TX 79968; verne@barium.physics.utep.edu

David L. Lambert
Department of Astronomy, University of Texas at Austin, Austin, TX 78712; dll@astro.as.utexas.edu

and

Kenneth H. Hinkle
National Optical Astronomy Observatory, P.O. Box 26732, Tucson, AZ 85726; khinkle@noao.edu
Received 2003 May 2; accepted 2003 May 15

ABSTRACT

The behavior of fluorine with metallicity has not yet been probed in any stellar population. In this work, we present the first fluorine abundances measured outside of the Milky Way from a sample of red giants in the Large Magellanic Cloud (LMC), as well the Galactic globular cluster ω Centauri. The fluorine abundances are derived from vibration-rotation transitions of HF using infrared spectra obtained with the Phoenix spectrograph on the Gemini South 8.1 m telescope. It is found that the abundance ratio of F/O declines as the oxygen abundance decreases. The values of F/O are especially low in the two ω Cen giants; this very low value of F/O probably indicates that ^{19}F synthesis in asymptotic giant branch (AGB) stars is not the dominant source of fluorine in stellar populations. The observed decline in F/O with lower O abundances is in qualitative agreement with what is expected if ^{19}F is produced via H- and He-burning sequences in very massive stars, with this fluorine then ejected in high mass-loss rate Wolf-Rayet winds. A quantitative comparison of observations with this process awaits results from more detailed chemical evolution models incorporating the yields from Wolf-Rayet winds. Perhaps of more significance is the quantitative agreement between the Galactic and LMC results with predictions from models in which ^{19}F is produced from neutrino nucleosynthesis during core collapse in supernovae of Type II. The very low values of F/O in ω Cen are also in agreement with neutrino nucleosynthesis models if the "peculiar" star formation history of ω Cen, with two to four distinct episodes of star formation, is considered.

Key words: galaxies: individual (Large Magellanic Cloud) — globular clusters: individual (ω Centauri) — nucleosynthesis — stars: abundances

1. INTRODUCTION

Unlike its neighbors in the periodic table, the nucleosynthetic origins of fluorine have remained somewhat obscure. This obscurity reflects a combination of theoretical and observational unknowns. The one stable isotope of fluorine, ^{19}F, is not easy to produce in stars, since it is readily destroyed by either proton or α-captures during many phases of stellar evolution. From an observational point of view, fluorine is difficult to detect spectroscopically. The only atomic lines that might be studied are the ground-state lines of F I, falling in the far-UV near 950 Å. The molecule HF is readily detectable in cool stars through vibration-rotation transitions that fall in the infrared near $\sim$2.3 μm. The HF pure rotational transitions are in the observationally challenging submillimeter region and are not easily exploited with current technology (Neufeld et al. 1997).

Attempts to account for fragmentary data on the abundance of fluorine in the Galaxy have focussed mostly on three proposed sources: (1) neutrino-induced spallation of a proton from ^{20}Ne following the core-collapse phase of a massive-star supernova (Woosley & Haxton 1988)—this is referred to as the ν-process (Woosley et al. 1990); (2) synthesis during He-burning thermal pulses on the asymptotic giant branch (AGB), as suggested by Jorissen, Smith, & Lambert (1992); or (3) production of ^{19}F in the cores of stars massive enough to be Wolf-Rayet stars at the beginning of their He-burning phase (Meynet & Arnould 2000). The relative importance of the three sources is undetermined theoretically and observationally. Indeed, it is not known if the leading contributor of fluorine is among the listed trio. Clues to the site of fluorine synthesis lie in the run of the fluorine abundance with metallicity in the Galaxy, and the fluorine abundances in different stellar populations.

To date, the only fluorine abundances measured in stars other than the Sun were provided by Jorissen et al. (1992), who analyzed a few Galactic K and M giants, and a larger number of *s*-process–enriched Galactic giants (spectral

[1] Based on observations obtained at the Gemini Observatory, which is operated by the Association of Universities for Research in Astronomy, Inc., under a cooperative agreeement with the NSF on behalf of the Gemini partnership: the National Science Foundation (United States), the Particle Physics and Astronomy Research Council (United Kingdom), the National Research Council (Canada), CONICYT (Chile), the Australian Research Council (Australia), CNPq (Brazil), and CONICET (Argentina).

[2] Based on observations obtained with the Phoenix infrared spectrograph, developed and operated by the National Optical Astronomy Observatory.

[3] Visiting Astronomer, Gemini South Observatory.

types MS, S, and N), but all were stars of near-solar metallicity. It may be assumed that the fluorine abundance of the K and M giants is unaffected by stellar evolution. To expand knowledge of fluorine abundances, we present fluorine abundance measurements in two stellar systems other than the Galaxy. We discuss red giants of the Large Magellanic Cloud (LMC) and two red giants in the Galactic globular cluster ω Centauri. These red giants are significantly more metal poor than the K and M giants analyzed by Jorissen et al. (1992) and provide information for the first time on how the fluorine abundance varies as a function of metallicity.

2. OBSERVATIONS

Fluorine abundances are derived in this study from high-resolution IR spectra obtained on the 8.1 m Gemini South telescope with the NOAO Phoenix spectrometer (Hinkle et al. 1998). A discussion of the observations and data reduction has appeared already in Smith et al. (2002) and details can be found there. Spectra pertinent to the present analysis are single-order echelle spectra imaged on a 1024 × 1024 InSb Aladdin II array and were obtained with an entrance slit defining the resolution, where $R = \lambda/\Delta\lambda = 50{,}000$ (∼4 pixels for Phoenix on Gemini South). The data were reduced to one-dimensional spectra using IRAF.

Spectra analyzed here were centered near a wavelength of 23400 Å and cover a 120 Å window. The HF 1–0 R9 line is included along with CO first-overtone vibration-rotation lines (Smith et al. 2002).

3. ANALYSIS

3.1. *Determining the Fluorine Abundances*

The stars observed for the HF line include nine red giant members of the LMC and two red giant members of the Galactic globular cluster ω Cen. All of the stars were analyzed recently—see Smith et al. (2002) for the LMC giants and Smith et al. (2000) for the ω Cen stars. In both studies, a combination of photometry (mostly IR) and high-resolution spectroscopy is used to derive the stellar parameters necessary for an abundance analysis: effective temperature ($T_{\rm eff}$), surface gravity (parameterized as log g), microturbulent velocity (ξ), and stellar metallicity. The same analysis techniques are used in both the LMC and ω Cen studies. We adopt the stellar parameters derived in the Smith et al. (2000, 2002) papers. In Table 1, we list the program stars, along with published values of $T_{\rm eff}$, log g, and microturbulence, as well as Fe and O abundances. The Fe and O abundances in the LMC giants are taken from Smith et al. (2002), with the uncertainties listed being the standard deviations from the average of the three Fe I and four OH lines used in the abundance determinations. The abundances of Fe and O for the ω Cen members and α Boo were taken from Smith et al. (2000). In this paper, we adopt the spectroscopic notations for presenting abundances, with $A(x) = \log [N(x)/N({\rm H})] + 12.0$ and $[x/y] = \log [N(x)/N(y)]_{\rm ProgramStar} - \log [N(x)/N(y)]_{\rm Standard}$.

Fluorine abundances listed in the last column of Table 1 are derived from spectrum synthesis of the HF 1–0 R9 line. We used a recent version of the LTE synthesis code MOOG (Sneden 1973). The model atmospheres employed in the abundance analyses are based on two different versions of the atmosphere code MARCS (Gustafsson et al. 1975). The LMC models were constructed with the SOSMARCS version (Plez, Brett, & Nordlund 1992; Edvardsson et al. 1993; Asplund et al. 1997), while the ω Cen giants use an older version of the original MARCS code. Cunha et al. (2002) compared synthetic spectra generated from both SOSMARCS and MARCS models and found no significant differences (in fact, almost unmeasurable differences) between the codes for temperatures in the range of the program stars studied here.

In addition to the metal-poor giants from the LMC and ω Cen, the nearby red giant α Boo was analyzed using the new IR spectral atlas from Hinkle, Wallace, & Livingston (1995). Although α Boo was included in the fluorine work by Jorissen et al. (1992), their analysis was based on an earlier IR spectrum that did not have as high a signal-to-noise ratio as the Hinkle et al. (1995) atlas. Stellar parameters for α Boo (Table 1) are from the recent analyses of Smith et al. (2000, 2002).

Sample comparisons of real with synthetic spectra are shown in Figure 1 for star LMC 1.27 and in Figure 2 for ROA 324 from ω Cen. These figures illustrate the quality of

TABLE 1

Program Star Parameters and Abundances

Star	$T_{\rm eff}$ (K)	log g	ξ (km s^{-1})	A(Fe)[a]	$A(^{16}{\rm O})$[a]	$A(^{19}{\rm F})$[a,b]
LMC 1.6	3760	+0.80	2.5	7.00 ± 0.10	8.02 ± 0.17	3.76
LMC 1.27	3550	+0.30	3.1	7.14 ± 0.13	8.24 ± 0.11	3.93
LMC 1.50	3550	+0.30	2.8	7.13 ± 0.05	8.29 ± 0.15	4.19
LMC 2.1158	3640	+0.40	2.5	7.16 ± 0.06	8.11 ± 0.15	3.62
LMC 2.3256	3680	+0.60	2.6	7.05 ± 0.09	8.22 ± 0.09	3.93
LMC 2.4525	3650	+0.50	3.0	7.05 ± 0.10	8.29 ± 0.13	4.01
LMC 2.5368	3650	+0.50	1.9	7.12 ± 0.10	8.26 ± 0.15	3.56
LMC NGC 2203 AM 1	3850	+0.60	3.3	6.83 ± 0.11	8.31 ± 0.13	4.06
LMC NGC 2203 AM 2	3700	+0.40	3.1	6.89 ± 0.07	8.20 ± 0.14	4.06
ω Cen ROA 219	3900	+0.70	1.7	6.25 ± 0.14	8.20[c]	3.16
ω Cen ROA 324	4000	+0.70	1.9	6.55 ± 0.20	8.28[c]	≤3.1
α Boo	4300	+1.70	1.6	6.78 ± 0.11	8.39[c]	4.10

[a] $A({\rm X}) = \log [n({\rm X})/n({\rm H})] + 12$.

[b] ^{19}F abundances are derived from synthesis of the HF(1–0) R9 line. We adopt the following parameters for this line: $\lambda_{\rm air} = 23357.75$ Å $\chi = 0.48$ eV, $gf = 1.11 \times 10^{-4}$, and $D_0({\rm HF}) = 5.82$ eV.

[c] These oxygen abundances are from the single [O I] 6300 Å line.

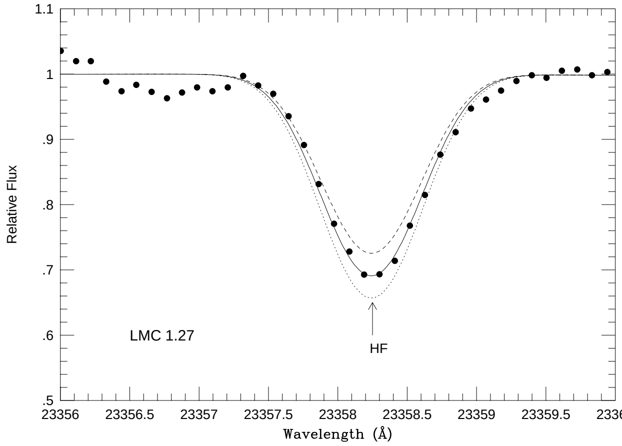

FIG. 1.—Observed and synthetic spectra for the star LMC 1.27. The synthetic spectra were calculated for $A(\mathrm{F}) = 3.83$, 3.93, and 4.03.

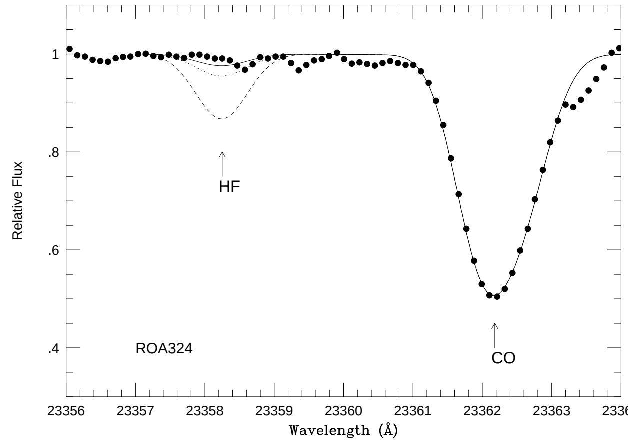

FIG. 2.—Observed and synthetic spectra for the ω Centauri giant ROA 324. Three fluorine abundances of, respectively, 3.10, 3.4, and 3.98 are presented. An upper limit fluorine abundance of $A(\mathrm{F}) = 3.10$ was adopted for this star.

the observed spectra and obtained fits. Note in the case of ROA 324 that HF is not detected. The lowest abundance shown in the figure is $A(F) = 3.10$, and we adopt this value as a conservative upper limit to the fluorine abundance (the line-profile depths at this abundance are just slightly greater than the noise level in the observed spectrum).

The sensitivity of the fluorine abundance to input stellar parameters was quantified by individually varying T_{eff}, surface gravity, and microturbulence to measure their separate effects on the derived abundances. A baseline model with $T_{\mathrm{eff}} = 3600$ K, $\log g = 0.50$, and $\xi = 2.5$ km s^{-1} was used. The following abundance differences were found for a R9 line having the same strength as in LMC 2.1158: $\Delta T_{\mathrm{eff}} = +70$ K gives $\Delta A(\mathrm{F}) = +0.14$ dex, $\Delta(\log g) = +0.3$ dex gives $\Delta A(\mathrm{F}) = +0.02$ dex, and $\Delta\xi = +0.5$ km s^{-1} gives $\Delta A(\mathrm{F}) = -0.03$ dex. These are typical stellar parameter uncertainties, and a quadrature sum of the abundance changes yields a combined uncertainty of 0.15 dex in the derived ^{19}F abundance due to the estimated errors.

3.2. *Reanalysis of the Older Fluorine Data*

In order to establish the behavior of fluorine with metallicity and across stellar populations, we add the only other available fluorine abundance measurements in the Galactic disk: these are the non–*s*-process–enriched K and M giants studied in Jorissen et al. (1992). We do not include the *s*-process–enriched AGB stars of spectral types MS, S, or C because Jorissen et al. (1992) found that ^{19}F is synthesized during He-burning thermal pulses, and this freshly produced fluorine is mixed to the surfaces of these AGB stars. Since our primary motivation here is to follow the general chemical evolution of fluorine with metallicity (using both Fe and O as metallicity indicators), inclusion of the self-polluted ^{19}F-rich AGB stars will obscure any metallicity trend.

A reanalysis of the Jorissen et al. (1992) abundances for the M giants was conducted, since the original results were derived from model atmospheres computed by Johnson, Bernat, & Krupp (1980). A comparison of models computed from the MARCS code and those of Johnson et al. (1980) reveals that, in the outer line-forming layers, the latter are slightly hotter ($\sim$50 K): this small difference has a small effect ($\sim$0.1 dex) on the derived fluorine abundances. The Jorissen et al. (1992) stellar parameters for these stars were taken from the papers by Smith & Lambert (1985, 1986, 1990) and, since these were also based mostly on the IR photometric T_{eff} scale, we adopt these same parameters but use MARCS model atmospheres to reanalyze the HF equivalent widths published by Jorissen et al. (1992).

Table 2 lists the K and M giants from Jorissen et al. (1992), along with their parameters and our derived Fe, O, and F abundances. Not only were the fluorine abundances recomputed with MARCS models, but also the iron and oxygen abundances using the published equivalent widths of Fe I and OH lines from Smith & Lambert (1985, 1986, 1990). In these earlier studies, the Fe I *gf*-values were "astrophysical," based upon an analysis of the K giant α Tau. The new abundances are based upon *gf*-values from the Kurucz & Bell (1995) line list. The effect of different model atmospheres and *gf*-values is small: the average differences, in the sense of new minus old is $A(\mathrm{Fe}) = +0.06$ and $A(\mathrm{O}) = -0.10$. The field K giants HR 5563 and HR6705 have fluorine abundances derived from the HF 1–0 R9 line, as in the LMC and ω Cen giants, while the cooler field M giants had the R13, R14, R15, and R16 lines measured. The comparison between the K and M giant ^{19}F abundances shows complete agreement, indicating that we have a homogeneous set of fluorine abundances for some 23 red giants across three stellar populations—the solar neighborhood, ω Cen, and the LMC.

3.3. *The Solar Fluorine Abundance*

Jorissen et al. (1992) pointed out that their sample of normal K and M giants with near-solar metallicities gave an average ^{19}F abundance somewhat larger than the solar abundance. The average abundance as discussed in Jorissen et al. (1992) sample of giants was $A(\mathrm{F}) = 4.69$. The solar abundance is somewhat uncertain: Anders & Grevesse (1989) quote a meteoritic abundance of $A(\mathrm{F}) = 4.48 \pm 0.06$ and a solar photospheric abundances (from HF lines of sunspots) of 4.56 ± 0.30.

Our reanalysis of the Jorissen et al. data presented in Table 2 yields slightly different abundances. Taking only those K and M giants with oxygen abundances in the range of $A(\mathrm{O}) = 8.7$–8.9 (with solar being 8.77, which is the value found using one-dimensional MARCS models as discussed by Allende Prieto, Lambert, & Asplund 2001), the average ^{19}F abundance is found to be 4.65 ± 0.07: marginally closer

TABLE 2
STARS REANALYZED FOR FLUORINE ABUNDANCES

Star	T_{eff} (K)	log g	ξ (km s^{-1})	A(Fe)[a]	$A(^{16}O)$[a]	$A(^{19}F)$[a]
HR 337	3800	+1.6	2.1	7.53 ± 0.12	8.75 ± 0.09	4.63 ± 0.08
HR 4483	3450	+0.8	2.0	7.55 ± 0.17	8.61 ± 0.11	4.53 ± 0.13
HR 5226	3650	+1.0	2.8	7.35 ± 0.15	8.83 ± 0.10	4.60 ± 0.08
HR 5563	4150	+1.9	2.0	7.27 ± 0.15	8.72 ± 0.15	4.66
HR 6705	3980	+1.9	2.0	7.27 ± 0.18	8.66 ± 0.18	4.67
HR 8775	3600	+1.2	2.0	7.55 ± 0.14	8.68 ± 0.10	4.56 ± 0.12
HD 96360	3550	+0.5	2.1	7.22 ± 0.17	8.82 ± 0.05	4.75 ± 0.05
HD 189581	3500	+0.5	2.1	7.17 ± 0.19	8.74 ± 0.09	4.60 ± 0.08
BD +06°2063	3550	+0.5	2.1	7.62 ± 0.11	8.64 ± 0.11	4.73 ± 0.13
BD +16°3426	3450	+0.5	2.0	7.32 ± 0.18	8.71 ± 0.06	4.72 ± 0.05
BD −13°4495	3600	+0.8	2.3	7.53 ± 0.16	8.52 ± 0.12	4.34 ± 0.11

[a] $A(X) = \log[n(X)/n(H)] + 12$. Adopted Solar abundances are $A(Fe) = 7.50$, $A(^{16}O) = 8.77$, and $A(^{19}F) = 4.55$.

to the solar values, but still larger. The eight disk giants have an average oxygen abundance of 8.78—within 0.01 dex of solar. In discussing stellar fluorine abundances, we adopt $A(F) = 4.55$ as the value of ^{19}F for the Sun, thus there is still a small 0.10 dex offset between the solar value and the average of the near-solar metallicity disk giants.

4. DISCUSSION

The measurements of fluorine abundances in three different stellar populations with differing metallicities hold clues to the origins of fluorine. It is recognized, of course, that evolution of an elemental abundance in a stellar system depends on factors other than simply the yields from the principal site of nucleosynthesis for the element. Such factors include the star formation history and the dispersal of stellar ejecta throughout a stellar population; consideration of these additional processes are argued to be important here when comparing fluorine abundances in the globular cluster ω Cen to the Milky Way and the LMC.

4.1. *The Behavior of Fluorine with Oxygen and Iron*

The first comparison of fluorine with oxygen and iron is shown in Figure 3: the top panel is A(F) versus A(O), and the bottom panel is A(F) versus A(Fe). Looking first at oxygen, it is clear from Figure 3 that the field K and M giant abundances are very close to solar. In addition, the metal-poor Galactic giant α Boo, with $A(O) = 8.38$ (or $[O/H] = -0.39$) has a near-solar F/O abundance ratio (represented by the solid line). Including the LMC red giants in the picture, one finds that, in general, they also scatter about the solar F/O line: the mean difference and standard deviation of the Galactic and LMC points about the solar F/O line is $+0.03 \pm 0.17$ dex. This scatter is very similar to that expected from the errors in the analysis. The striking deviations from the solar F/O line are the two ω Cen giants, with both falling well below a solar F/O abundance ratio: the upper limit in ROA 324 is a firm limit, as shown in Figure 2. As will be discussed in § 4.2.3, the star formation history in ω Cen is very different from that of the Milky Way and the LMC and will lead to a simple explanation for the low fluorine abundances in this system.

The comparison between F and Fe in the bottom panel of Figure 3 shows more scatter about a scaled solar line for the disk and LMC giants. In this case, the mean difference and standard deviation is $+0.02 \pm 0.30$ dex, almost twice as large as the scatter found about the F/O line. Although one of the ω Cen giants has an F/Fe ratio close to solar, the conservative upper limit for ROA 324 is still significantly subsolar in F/Fe.

Figure 4 shows the relation of [F/O] using oxygen as the metallicity indicator. The use of oxygen removes supernovae of Type Ia as a contributing source, since iron can have SN Ia's as a dominant parent in some stellar populations; none of the possible sites put forth as ^{19}F sources involve these types of supernovae. Inspection of this figure reveals a gradual decrease in the average [F/O] value when going from the near-solar metallicity Galactic stars to the lower metallicity LMC giants and α Boo.

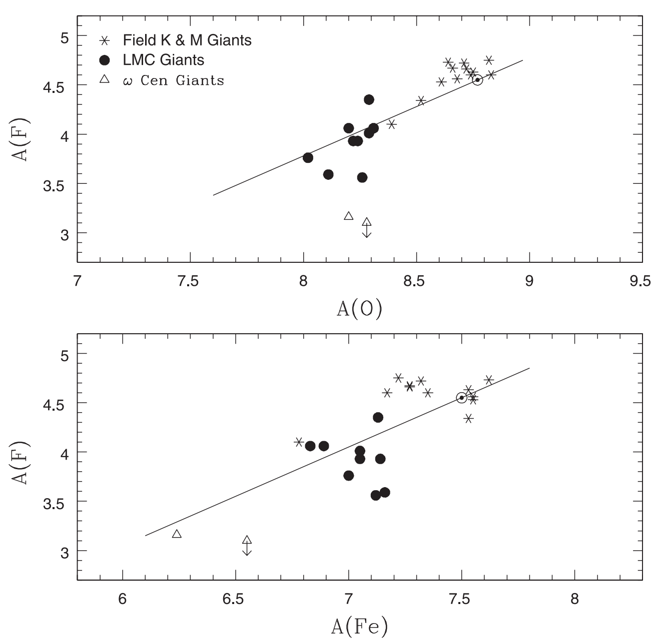

FIG. 3.—*Top*: Logarithmic abundances of fluorine vs. oxygen. The solar symbol is shown, and the solid line illustrates a solar F/O abundance ratio. *Bottom*: Similar to the top, except fluorine is plotted vs. iron. The A(F) vs. A(O) results show slightly less scatter about a solar F/O line than the A(F) vs. A(Fe) values about a solar F/Fe line. Note the very low F/O ratios in the ω Cen giants.

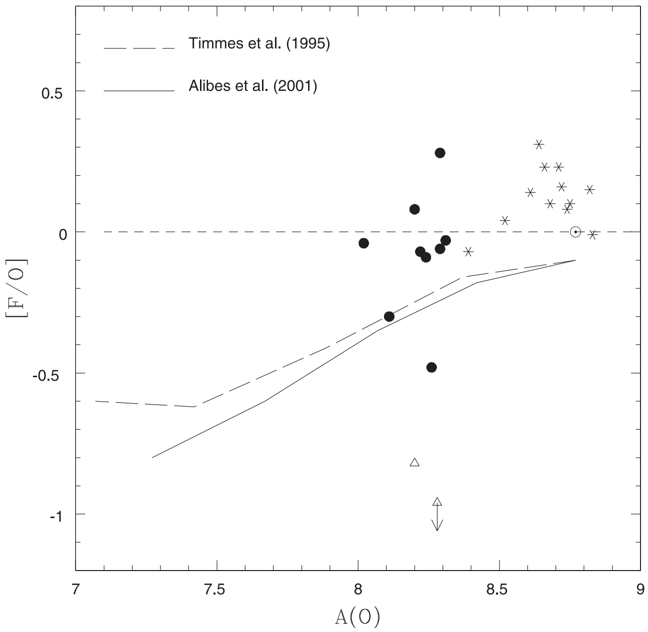

Fig. 4.—Fluorine-to-oxygen abundance ratios, shown as [F/O], vs. A(O), with the horizontal dashed line depicting a solar F/O ratio. The symbols for the various stellar systems are the same as in Fig. 3. The lines are predictions from chemical evolution models in which the ν-process contributes to the synthesis of ^{19}F: the dashed line is from Timmes et al. (1995), and the solid line is from Alibés et al. (2001).

The continuous lines plotted in Figure 4 are predictions from chemical evolution models by Timmes, Woosley, & Weaver (1995) and Alibés, Labay, & Canal (2001) for the behavior of [F/O] with oxygen for the ν-process yields as given by Woosley & Weaver (1995). In both models, the [F/O] values are slightly subsolar at solar metallicity by approximately -0.1 dex. As pointed out by Alibés et al. (2001), ^{19}F production is very sensitive to the neutrino fluxes and spectra, so the yield is uncertain; a 0.1 dex offset from solar is probably not significant. Timmes et al. (1995) show (in their Fig. 10) the effects of factor 2 variations in the mass of ejected fluorine, and we have used their mean curve. We note that quantitative chemical evolution model results for F production during the Wolf-Rayet (WR) phase are not available in the literature and thus are not discussed here.

4.2. *The Pros and Cons of the Sites for the Chemical Evolution of Fluorine*

As discussed in § 1, three main sites have been put forth as possible net ^{19}F producers: (1) operation of a neutron source during He-burning thermal pulses in AGB stars, (2) mass loss from WR stars during their phase of He-burning, and (3) the ν-process in supernovae of Type II. In our discussion of the behavior of fluorine as a function of metallicity, we use oxygen as the " appropriate " metallicity indicator.

4.2.1. *AGB Stars*

Jorissen et al. (1992) probed the conditions under which ^{19}F could be produced as a result of a combination of α-captures originating on ^{14}N, a neutron source, and proton captures, all occurring during thermal pulses in AGB stars. Although they could explain the enhanced fluorine abundances observed in the s-process–enriched and ^{12}C-rich stars, they did not make detailed predictions about the chemical evolution of ^{19}F. Due to the longer timescales of AGB evolution, Jorissen et al. (1992) did argue that fluorine would likely follow the behavior of iron, which also has a long timescale component arising from SN Ia's, thus [F/Fe] would be $\sim$0. Examination of Figure 3 shows that the scatter about the F/Fe line is almost twice as large as the scatter about the F/O line, as discussed previously. This suggests that perhaps AGB stars are not the place to look for major fluorine production. In this instance, the ω Cen giants enter the picture as potentially crucial points, due to the large s-process abundances found in many of the ω Cen members: a result usually interpreted as showing an especially large degree of AGB enrichment contributing to the chemical evolution within ω Cen. In such a picture, the ω Cen giants should exhibit enhanced fluorine abundances, but show completely opposite behavior.

4.2.2. *Wolf-Rayet Stars*

In massive stars, ^{19}F can be produced during the pre-explosive nucleosynthesis in the helium shell from reaction sequences not involving neutrinos, but by a series of thermonuclear reactions. The synthesis of ^{19}F by these reactions consists of two modes, one consisting of a CNO H-burning sequence and the other consisting of a set of He-burning sequences. In the CNO H-burning sequence, a series of proton captures and β-decays, initiated on ^{14}N, leads to a finite abundance of ^{19}F, with ^{19}F$(p,\alpha)^{16}$O being the destructive reaction. During He-burning, the sequences to produce ^{19}F begin with an α-capture on ^{14}N and conclude with an α-capture on ^{15}N [^{15}N$(\alpha,\gamma)^{19}$F]; this series of reactions also involves neutron and proton captures, with the neutrons and protons supplied by ^{13}C$(\alpha,n)^{16}$O and ^{14}N$(n,p)^{14}$C, respectively. The possible production of fluorine via these reactions in massive stars was first investigated by Woosley & Weaver (1995), who concluded that the above mentioned reactions could not reproduce the abundance of fluorine at solar metallicity. More recently, however, Meynet & Arnould (2000) investigated the role that WR stars may play in the chemical evolution of fluorine by adopting more modern reaction rates (NACRE compilation) coupled with more extreme mass-loss rates and conclude that production of fluorine in WR stars could explain the solar fluorine abundances.

The crucial point emphasized in the Meynet & Arnould (2000) study concerning the chemical evolution of fluorine is that any ^{19}F produced either through the various proton or α-capture reactions must be removed from the stellar interior to avoid destruction. In order for massive stars to be significant contributors to net fluorine production, they must undergo extensive mass loss; the requirement of large mass-loss rates needed to eject the fluorine before its destruction is met by the WR stars. Meynet & Arnould point out that WR mass loss is very metallicity dependent, and that the numbers of WR stars at low metallicities are also very small. Thus they predict that fluorine yields from WR stars will exhibit a strong dependence on metallicity, with a very small to negligible yield at low metallicity, and increasing ^{19}F yields toward solarlike metallicities. Our results as shown in Figure 4 with [F/O] plotted versus A(O) do show a decline in the F/O abundance ratio as the oxygen abundance decreases, as would be expected qualitatively from arguments about the low production of fluorine at low metallicities from WR stars. At this time, it is not possible to compare quantitatively the observed abundances with predictions from WR-wind models because there are no published model values of how the abundance of fluorine varies with oxygen.

4.2.3. *Massive Stars and the ν-Process*

Perhaps at this time, the leading use for our data on fluorine is as a test of the proposal that fluorine is primarily synthesized by the ν-process in SN II. This is possible now because predicted yields for ^{19}F (and ^{16}O, a reference element for SN II nucleosynthesis) for massive stars of different initial metallicities were supplied by Woosley & Weaver (1995), while Timmes et al. (1995), Goswami & Prantzos (2000), and Alibés et al. (2001) have incorporated these yields into models of Galactic chemical evolution, producing predictions of fluorine abundances as a function of the oxygen abundance.

The chemical evolution models, with ν-process produced ^{19}F, predict that the [F/O] declines fairly steadily as the oxygen abundance declines; this is illustrated in Figure 4 for two of the published studies (Timmes et al. 1995 and Alibés et al. 2001), with both chemical models agreeing quite well. The rate of decrease of [F/O] with A(O) is similar to the results for the Galactic and LMC stars, with an apparent small offset between model and observed [F/O]. Recall that there still remains a small uncertainty in the local Galactic fluorine abundance, which can be seen in Figure 4 as the offset of the solar point from the mean of the local K and M giants. The slow decline in [F/O] with A(O) found in the Galactic and LMC stars is fitted well by the ν-process models.

The consistency between the observed F/O ratios and the model values is not found for the giants from ω Cen for which $[F/O] = -0.82$ and ≤ -0.94. To understand this apparent inconsistency, it is necessary to recognize that ω Cen is a very different type of stellar system compared with the LMC or the Milky Way. Although described as a globular cluster, ω Cen is far from a typical Galactic cluster. It is not only the most massive globular cluster but, in contrast to other clusters, there is a large spread ($\sim$1.5 dex) in metallicity among its members. In other globular clusters (except, perhaps, M22), the star-to-star spread in Fe abundance is 0.05 dex or less. No detailed picture of the formation and evolution of a globular cluster yet exists, but it is thought that an initial generation of stars polluted metal-poor gas from which later generations of stars formed. There may have been three or four star formation episodes in ω Cen (Pancino et al. 2000), although the metal-poor first generation of stars far outnumber the later generations of more metal-rich stars (Norris, Freeman, & Mighell 1996; Suntzeff & Kraft 1996; Norris et al. 1997). We suppose that this scenario of a few, well-separated star formation episodes, which ended many billions of years ago, applies to ω Cen. This contrasts with the LMC and the Galaxy that continue to undergo star formation.

Consider the following simplest case to describe ω Cen. Ejecta from a first generation of stars mixes to differing degrees with a reservoir of very metal-poor gas. Pockets of gas of differing heavy-element enrichment will result. Stars comprising a later generation that formed from these pockets will have a spread in heavy-element abundances, as observed in ω Cen. Yet, abundance ratios—say, F/O—will be very similar for all pockets, as long as the primordial gas was severely underabundant in the elements comprising a ratio. In the case of an abundance ratio, which for SN II ejecta is dependent on the initial metallicity, the abundance ratio will stand out as anomalous when judged against the run of the abundance ratio versus metallicity established from stars that form from gas that has undergone many episodes of star formation where the stellar ejecta become well mixed with the interstellar medium (as is probably the case for the Galactic and LMC stars). Abundance ratios insensitive to the initial metallicity of SN II will appear normal, or nearly so, relative to the Galactic standards. The most metal-poor stars in ω Cen have oxygen abundances near $A(O) \sim 7.3$ (Smith et al. 2000). If supernovae of Type II with this initial abundance of oxygen dominated the nucleosynthesis of fluorine via the ν-process, as predicted by our simple picture, then the later generation of ω Cen stars would form from gas having $[F/O] \sim -0.8$ (using ν-process model predictions as illustrated in Fig. 4). This is confirmed by the abundance results for the observed ω Cen stars.

As noted above, our scenario predicts "anomalous" abundance ratios for all ratios that are dependent on the initial metallicity of the SN II. Copper is such an example. Significantly, the [Cu/Fe] from ω Cen giants (Cunha et al. 2002) is constant over the [Fe/H] range probed ($[Fe/H] = -2$ to -0.8) and falls below its corresponding values in Galactic halo stars.

5. CONCLUSIONS

We present the first fluorine abundance measurements outside of the Milky Way, in the LMC, and the first measurements in a globular cluster (ω Cen). It is found that the F/O abundance ratios decline as metallicity (taken as the oxygen abundance) decreases. This decline is moderate for the LMC (or α Boo) relative to the near-solar metallicity Galactic disk stars, with the average value of [F/O] in the LMC being $\sim$0.2 dex lower at an oxygen abundance that is about 0.5 dex lower. The values of [F/O] are much lower still in the two ω Cen giants ($[F/O] \sim -0.9$) at a similar oxygen abundance as those in the LMC sample.

The very low values of [F/O] found in the two ω Cen stars suggest that AGB stars do not play a dominant role in the global chemical evolution of fluorine in a stellar population. Because of the large *s*-process elemental abundances found in the more metal-rich ω Cen stars (as typified by the two ω Cen targets studied here), a relatively large AGB contribution to the chemical evolution within ω Cen is inferred. If AGB stars have had such a large impact on the chemical evolution, it would be expected that this would result in elevated values of [F/O], instead of the very low values observed.

Both ^{19}F production sites that involve massive stars, either via thermonuclear reactions with the synthesized fluorine being ejected in the high dM/dt stellar winds of a WR star, or from neutrino spallation off of ^{20}Ne during core collapse in SN II, predict lower values of [F/O] at lower oxygen abundances. With the results presented here, it is not possible to test conclusively whether WR winds or the ν-process might dominate the chemical evolution of ^{19}F. This test must await quantitative chemical evolution models incorporating the yields from WR winds. In the meantime, it should be noted that the decline in [F/O] versus A(O) observed in the Galactic and LMC stars agrees reasonably well with the chemical evolution models using ν-process yields for ^{19}F.

The very low values of [F/O] indicated for the ω Cen stars seem, at first glance, at odds with the ν-process models. This apparent discrepancy is resolved when the very different star formation history in ω Cen, when compared with the Milky Way and the LMC, is considered.

We thank G. Meynet for helpful discussions. This work is supported in part by the National Science Foundation through AST 99-87374 (V. V. S.) and NASA through NAG 5-9213 (V. V. S.). D. L. L. acknowledges the support of the Robert A. Welch Foundation of Houston, Texas.

REFERENCES

Alibés, A., Labay, J., & Canal, R. 2001, A&A, 370, 1103
Allende Prieto, C., Lambert, D. L., & Asplund, M. 2001, ApJ, 556, L63
Anders, E., & Grevesse, N. 1989, Geochim. Cosmochim. Acta, 53, 197
Asplund, M., Gustafsson, B., Kiselman, D., & Eriksson, K. 1997, A&A, 318, 521
Cunha, K., Smith, V. V., Suntzeff, N. B., Norris, J. E., Da Costa, G. S., & Plez, B. 2002, AJ, 124, 379
Edvardsson, B., Andersen, J., Gustafsson, B., Lambert, D. L., Nissen, P. E., & Tomkin, J. 1993, A&A, 275, 101
Goswami, A., & Prantzos, N. 2000, A&A, 359, 191
Gustafsson, B., Bell, R. A., Eriksson, K., & Nordlund, A. 1975, A&A, 42, 407
Hinkle, K. H., Cuberly, R., Gaughan, N., Heynssens, J., Joyce, R., Ridgway, S., Schmitt, P., & Simmons, J. E. 1998, Proc. SPIE, 3354, 810
Hinkle, K. H., Wallace, L., & Livingston, W. 1995, Infrared Atlas of the Arcturus Spectrum, 0.9–5.3 μm (San Francisco: ASP)
Johnson, H. R., Bernat, A. P., & Krupp, B. M. 1980, ApJS, 42, 501
Jorissen, A., Smith, V. V., & Lambert, D. L. 1992, A&A, 261, 164
Kurucz, R. L., & Bell, B. 1995, CD-ROM 23, Atomic Line Data (Cambridge: SAO)
Meynet, G., & Arnould, M. 2000, A&A, 355, 176
Neufeld, D. A., Zmuidzinas, J., Schilke, P., & Phillips, T. G. 1997, ApJ, 488, L141
Norris, J. E., Freeman, K. C., Mayor, M., & Seitzer, P. 1997, ApJ, 487, L187
Norris, J. E., Freeman, K. C., & Mighell, K. J. 1996, ApJ, 462, 241
Pancino, E., Ferraro, F. R., Bellazzini, M., Piotto, G., & Zocalli, M. 2000, ApJ, 534, L83
Plez, B., Brett, J. M., & Nordlund, A. 1992, A&A, 256, 551
Smith, V. V., et al. 2002, AJ, 124, 3241
Smith, V. V., & Lambert, D. L. 1985, ApJ, 294, 326
———. 1986, ApJ, 311, 843
———. 1990, ApJS, 72, 387
Smith, V. V., Suntzeff, N. B., Cunha, K., Gallino, R., Busso, M., Lambert, D. L., & Straniero, O. 2000, AJ, 119, 1239
Sneden, C. 1973, ApJ, 184, 839
Suntzeff, N. B., & Kraft, R. P. 1996, AJ, 111, 1913
Timmes, F. X., Woosley, S. E., & Weaver, T. A. 1995, ApJS, 98, 617
Woosley, S. E., Hartmann, D. H., Hoffman, R. D., & Haxton, W. C. 1990, ApJ, 356, 272
Woosley, S. E., & Haxton, W. C. 1988, Nature, 334, 45
Woosley, S. E., & Weaver, T. A. 1995, ApJS, 101, 181